Molecular Template for a Voltage Sensor in a Novel K^+ Channel. III. Functional Reconstitution of a Sensorless Pore Module from a Prokaryotic Kv Channel

Jose S. Santos, Sergey M. Grigoriev, and Mauricio Montal

Section of Neurobiology, Division of Biological Sciences, University of California, San Diego, La Jolla, CA 92093

KvLm is a prokaryotic voltage-gated K^+ (Kv) channel from *Listeria monocytogenes*. The sequence of the voltage-sensing module (transmembrane segments S1-S4) of KvLm is atypical in that it contains only three of the eight conserved charged residues known to be deterministic for voltage sensing in eukaryotic Kv's. In contrast, the pore module (PM), including the S4-S5 linker and cytoplasmic tail (linker-S5-P-S6-C-terminus) of KvLm, is highly conserved. Here, the full-length (FL)-KvLm and the KvLm-PM only proteins were expressed, purified, and reconstituted into giant liposomes. The properties of the reconstituted FL-KvLm mirror well the characteristics of the heterologously expressed channel in *Escherichia coli* spheroplasts: a right-shifted voltage of activation, micromolar tetrabutylammonium-blocking affinity, and a single-channel conductance comparable to that of eukaryotic Kv's. Conversely, ionic currents through the PM recapitulate both the conductance and blocking properties of the FL-KvLm, yet the KvLm-PM exhibits only rudimentary voltage dependence. Given that the KvLm-PM displays many of the conduction properties of FL-KvLm and of other eukaryotic Kv's, including strict ion selectivity, we conclude that self-assembly of the PM subunits in lipid bilayers, in the absence of the voltage-sensing module, generates a conductive oligomer akin to that of the native KvLm, and that the structural independence of voltage sensing and PMs observed in eukaryotic Kv channels was initially implemented by nature in the design of prokaryotic Kv channels. Collectively, the results indicate that this robust functional module will prove valuable as a molecular template for coupling new sensors and to elucidate PM residue–specific contributions to Kv conduction properties.

The Journal of General Physiology

Downloaded from http://rupress.org/jgp/article-pdf/132/6/651/1786737/jgp_200810077.pdf by guest on 09 February 2026

INTRODUCTION

In voltage-gated K^+ (Kv) channels four subunits assemble (MacKinnon, 1991), each contributing one quarter of the pore (S5-P-S6) and a full voltage sensor (S1-S4) module (Jiang et al., 2003; Cuello et al., 2004; Bezanilla, 2005; Chapman and VanDongen, 2005; Long et al., 2005a). In the crystal structure (Long et al., 2005a), as well as in a model in a lipid bilayer (Jogini and Roux, 2007), the four sensor modules of the rodent Kv 1.2 (pdb 2A79) sit peripherally to the pore, one never touching the other. Such configuration restricts surface contact between pore and sensor only to a hydrophobic face of S4 and a hydrophobic face of S5 in the neighboring subunit. The near spatial independence of pore and sensor modules allows for largely unconstrained, independent module evolution and therefore maximum coupled-module diversity. These considerations posit the notion that each module may fold independently in the absence of the other. It is therefore not surprising that the two modules have been found to naturally occur and function as separate units, for example a voltage sensor coupled to an enzyme (Ci-VSP) (Murata et al., 2005) or on its own (Hv) (Ramsey et al., 2006; Sasaki et al., 2006) and a pore module (PM) in a non-voltage–gated channel (Schrempf et al., 1995; Cuello et al., 1998; Cortes et al., 2001; Jiang et al., 2002b, 2002a; Kuo et al., 2003; Kuo et al., 2007). These findings clearly validate this laboratory's previously proposed (Greenblatt et al., 1985; Montal, 1990; Patten et al., 1999) evolutionary modularity of the voltage sensor and PM: "a unit of interacting components that operates in an integrated (interdependent) but relatively context-insensitive manner and therefore behaves relatively invariantly in different contexts" (Schlosser and Wagner, 2004). But the discovery of sensors that conduct (Hv) (Ramsey et al., 2006; Sasaki et al., 2006) and of PMs that sense voltage and even inactivate (e.g., a potassium-selective channel gated by H^+ [KcsA] [Gao et al., 2005; Cordero-Morales et al., 2007] or by Ca^{2+} [MthK] [Kuo et al., 2007])

Correspondence to Mauricio Montal: mmontal@ucsd.edu

J.S. Santos' present address is Dept. of Biochemistry, University of Chicago, Chicago, IL 60637.

Abbreviations used in this paper: FL, full-length; HMM, hidden Markov model; KcsA, potassium-selective pH-gated channel from streptomyces lividans; Kv, voltage-gated K^+; KvAP, Kv channel from *Aeropyrum pernix*; KvLm, Kv channel from *Listeria monocytogenes*; PM, pore module; SN, supernatant; TBA, tetrabutylammonium; VSM, voltage sensor module.

The online version of this article contains supplemental material.

© 2008 Santos et al. This article is distributed under the terms of an Attribution–Noncommercial–Share Alike–No Mirror Sites license for the first six months after the publication date (see http://www.jgp.org/misc/terms.shtml). After six months it is available under a Creative Commons License (Attribution–Noncommercial–Share Alike 3.0 Unported license, as described at http://creativecommons.org/licenses/by-nc-sa/3.0/).

The Rockefeller University Press $30.00
J. Gen. Physiol. Vol. 132 No. 6 651–666
www.jgp.org/cgi/doi/10.1085/jgp.200810077

in the absence of a sensor, shattered the dogma that sensors sense and pores conduct and questions who does what in Kv channels? The answer to this question is especially relevant given that new properties emerge in naturally decoupled modules, as evident from blocking experiments and gating charge measurements that clearly demonstrated that voltage sensors in the context of intact Kv channels do not conduct ions (Bezanilla, 2002).

In Kv channels of prokaryotic origin, the sequence diversity of both voltage sensor modules (VSMs) and PMs is expected to be larger than in eukaryotes given the proposed additional roles that these modules play in bacteria (Kuo et al., 2005). A pairwise sequence comparison of an alignment of 87 candidate prokaryotic Kv channels confirms this expectation and shows that sequence identity conservation is markedly lower in the sensor than PM (Fig. S1, A–C, available at http://www.jgp.org/cgi/content/full/jgp.200810077/DC1). A direct inference from these observations is that voltage sensors and especially PMs from Kv channels of bacterial origin may exhibit greater structural plasticity to adapt to each other than their eukaryotic counterparts that have been constrained ("glued" together) by additional posttranslational modifications that confer additional features to the sensor–pore assembly, for example, localized and/or targeted subcellular or cellular expression (Cai et al., 2006; Park et al., 2008). Such specialization nonetheless renders the primary function of each module largely untouched. This is a plausible expectation given that residues shown to facilitate the hinge rotation that gates the pore open in prokaryotic and eukaryotic Kv channels alike (Fig. 1, A and B) are conserved (Magidovich and Yifrach, 2004; Ding et al., 2005; Seebohm et al., 2006; Hardman et al., 2007), as well as by the documented "portability" of sensor and PMs in chimeric constructs (Cao et al., 1995; Patten et al., 1999; Lu et al., 2002; Caprini et al., 2005; Alabi et al., 2007).

Collectively, the functional and structural information available suggest that PMs from Kv channels across all kingdoms of life fold into functional K^+-selective channels with gating dynamics similar to those exhibited by the same pore when controlled by the native sensor. A sensor-less Kv will inform on which Kv full-length (FL) channel properties are inherent to the pore alone and which are conferred by the sensor to the pore. Of special interest is to define the extent of gating cooperativity of the four subunits in the absence of a gating control, presumably enlightening the last structural transition in the pore preceding the start of ion conduction (Hoshi et al., 1994; Zagotta et al., 1994a, 1994b; Aggarwal and MacKinnon, 1996; Schoppa and Sigworth, 1998a, 1998b, 1998c). If any component of the sensor were essential to gate the Kv channel pore in a concerted manner, single-channel current measurements of the sensor-less construct should be paved with intermediate conduction states arising from the activation of one, two, or three pore subunits (Chapman and VanDongen, 2005). In eukaryotic channels in which the sensor was disconnected from the pore by means of mutations in the S4 segment of the VSM, the transition remained concerted but pore opening became largely voltage independent (Smith-Maxwell et al., 1998a, 1998b; Bao et al., 1999; Ledwell and Aldrich, 1999). Guided by this laboratory's previous attempt (Caprini et al., 2001) and by others (Lu et al., 2001; Caprini et al., 2005), successful chimeric design between a sensor from a fly and a pore from a bacterium and by the crystal structure of Kv 1.2, we successfully extracted the sensor from Kv channel from *Listeria monocytogenes* (KvLm) (Lundby et al., 2006; Santos et al., 2006), a prokaryotic Kv channel, thereby beginning gene transcription at the S4-S5 linker to generate a K^+-selective channel with the single-channel conductance and ion selectivity of the FL Kv channel. We discovered that indeed the VSM in Kv channels is the "gatekeeper" (Armstrong, 2003) and that concerted pore opening only requires sensor input at subthreshold membrane potentials.

MATERIALS AND METHODS

Sequence Alignment

New candidate bacterial Kv channel sequences were identified from hits of a BLAST (tblastn) search of all bacterial genomes at the National Center for Biotechnology Information database (http://www.ncbi.nlm.nih.gov/sutils/genom_table.cgi) using the *Shaker* Kv channel (Sh, *Drosophila melanogaster*, gi 13432103) sequence as query and added to an existing alignment of 54 sequences from bacterial genomes (Santos et al., 2006). A new master alignment was generated with Clustal X (v.1.83) (Thompson et al., 1997) using the Gonnet PAM series of protein weight matrices (Gonnet et al., 1992), refined by minimal manual adjustments and filtered in Jalview (Clamp et al., 2004) to include no sequences sharing >90% sequence pairwise identity. Using the structural information available for Kv channel from *Aeropyrum pernix* (KvAP) (Jiang et al., 2003; Cuello et al., 2004) as a ruler, the transmembrane segment boundaries for all 87 sequences in the alignment were identified and used to remove the sequences of the amino and carboxy termini and to break the alignment into two parts: an alignment of the VSM (S1-S4) and an alignment of the PM (S4-$S5_{linker}$-S5-P-S6). A profile hidden Markov model (HMM) (Eddy, 1998) for the PM alignment was constructed using a web server application (http://bioweb.pasteur.fr/seqanal/interfaces/hmmbuild.html). The consensus sequence generated by the HMM was converted to an HMM logo using a web server application (http://logos.molgen.mpg.de/cgi-bin/logomatm.cgi) (Fig. 1 A). To compare sequence conservation between the PM sequences of bacterial Kv channels and those of other potassium-selective pores with available structural information, the PM sequences of KcsA (gi 13399712), a bacterial pH-gated potassium-selective channel (Schrempf et al., 1995; Cuello et al., 1998), and of KCNA2, a Kv channel from rat (Kv1.2, sp P63142), were aligned by ClustalX with the 87-PM sequences from Kv bacterial origin. The aligned sequences of KvLm (gi 16411529), KvAP (gi 14601099), Kv 1.2, and KcsA were extracted from this alignment (Fig. 1 B).

Downloaded from http://rupress.org/jgp/article-pdf/132/6/651/1786737/jgp_200810077.pdf by guest on 09 February 2026

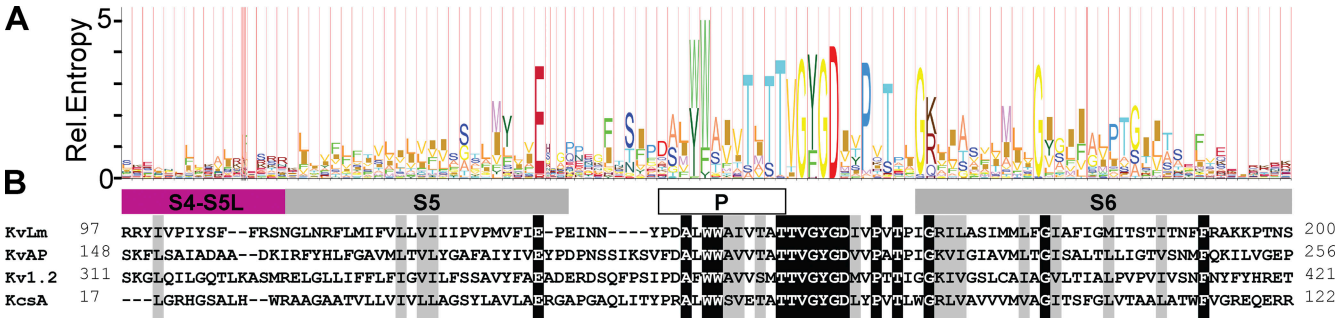

Figure 1. Sequence conservation in the PM of bacterial Kv channels. (A) An HMM logo for the PM sequence alignment, extracted from an alignment of 85 FL sequences of candidate bacterial Kv's with the sequences of KvAP and KvLm sharing a maximum of 90% pairwise sequence similarity (BLOSUM 62), reports the scaled amino acid frequency distribution at each position in the PM sequence. (B) The conservation of the PM sequence in Kv channels is shown in an alignment of PM sequences of two prokaryotic Kv channels (KvLm and KvAP) with those from a prokaryotic K^+ channel lacking a formal VSM (KcsA) and an eukaryotic Kv channel (Kv 1.2). Sequence identities and similarities are colored with a black and gray background.

Gene Cloning, Overexpression, Purification, and Reconstitution

The gene-encoding FL-KvLm was PCR cloned from *L. monocytogenes* eGDE genomic DNA (provided by P. Cossart, Institute Pasteur, Paris, France) and inserted into the *Escherichia coli* protein expression vector pQE-70 (QIAGEN) between the SphI and BglII restriction endonuclease sites. The SphI site was eliminated by site-directed mutagenesis using the QuikChange kit (QIAGEN) so as to replace the histidine residue encoded by the SphI sequence with the native KvLm aspartic acid residue. This is the only difference between the clone used in this study and that used for KvLm expression in spheroplasts (Lundby et al., 2006; Santos et al., 2006). To generate the KvLm-PM construct in which the sensor is clipped out, the KvLm gene was PCR amplified starting at residue R98 and cloned into the SphI and BglII restriction sites in pQE-70. Expression of FL-KvLm and KvLm-PM genes from these constructs generates proteins with a six-histidine C-terminal tag with calculated molecular weights of 29.7 kD (FL-KvLm) and 18.2 kD (KvLm-PM). Channel protein was expressed in *E. coli* XL-1 Blue cells (Agilent Technologies), grown in NaLM (Epstein and Kim, 1971) media (10 g/L Bacto-tryptone [DIFCO], 5 g/L yeast extract [DIFCO], and 115 mM NaCl [Thermo Fisher Scientific], pH 7.4) to an OD_{550} of 0.8–0.9 and induced with 0.5 mM isopropyl-β-D-thiogalactopyranoside for 3–4 h at 37°C. Cells were harvested by centrifugation at 9,000 *g* for 20 min at 4°C, resuspended in ice-cold 100 mM KCl, 5 mM NaCl, 50 mM MOPS, pH 7.0, containing 1 mg/ml lysozyme and protease inhibitors (1 mM PMSF, 2 µM leupeptin A, 2 µM pepstatin), and lysed by sonication on ice for 5 min, using 30-s on/30-s off cycles. All procedures from here on forth were performed on ice or at 4°C unless otherwise indicated. Unbroken cell and inclusion bodies were removed by centrifugation at 12,000 *g* for 15 min. Membranes were collected from the supernatant (SN) by centrifugation at 110,000 *g* for 45 min and resuspended in 100 mM K_2HPO_4 (KPi) and 5 mM NaCl, pH 8.0. Membranes were solubilized in the aforementioned buffer in the presence of 20 mM (1%) n-Dodecyl-β-D-maltopyranoside (DDM; Acros Organics) for 2 h. Insoluble material was removed by ultracentrifugation at 85,000 *g* for 45 min. To the SN an additional 200 mM KCl (400 mM K total) and 10 mM imidazole was added and mixed well before batch incubation with Ni-NTA agarose resin (QIAGEN) for 1.5 h. Resin protein slurry was poured onto a disposable column (Bio-Rad Laboratories) and unbound protein was washed off with 10-column volumes of 20 mM imidazole in 100 mM KPi, 200 mM KCl, and 10 mM (0.5%) DDM, pH 8.0. FL-KvLm and KvLm-PM were eluted at 300 mM imidazole in an otherwise same buffer composition. The typical yield of FL-KvLm and KvLm-PM was ∼0.3 and 1.0 mg/L.

Giant proteoliposomes, several micrometers in diameter, can be readily prepared by repeated cycles of freezing and thawing, or by dehydration and subsequent rehydration. Several variations of this method are widely used (Darszon et al., 1980; Saimi et al., 1999; Cortes et al., 2001; Grigoriev et al., 2004; Cordero-Morales et al., 2006a, 2006b). Their spherical configuration is documented to favor the assembly of a single population of oriented channels in the reconstituted bilayer, which is superior to that generated by the planar bilayer geometry (for example Ruta et al., 2003, 2005; Nimigean et al., 2004; Cordero-Morales et al., 2006a, 2006b). Purified KvLm proteins were reconstituted into asolectin (L-α-phosphatidylcholine; Type IV-S; Sigma-Aldrich) liposomes (25 mg/ml) suspended in 200 mM KCl and 5 mM HEPES, pH 7.0, by incubating the mixture (lipid/protein mass ratios between 15 and 50 to 1) on ice for 15 min, followed by overnight dialysis in a 500-µl Slide-a-Lyzer dialysis cassette (Thermo Fisher Scientific) with a 3.5-kD molecular weight cutoff against 1 L of dialysis buffer (200 mM KCl and 5 mM HEPES, pH 7.0). The dialysis buffer was replaced in full after 1 h and again after 12 h. The total dialysis time was ∼16 h. The detergent-free proteoliposome mixture was then centrifuged to remove insoluble material, and the SN was distributed into 20-µg protein aliquots that were either frozen immediately at −80°C or used to make giant proteoliposomes for patching. Giant proteoliposomes were made by supplementing a dialysis aliquot with 20–40 µl of asolectin liposomes (25 mg/ml), vortexing briefly, and spotting 20-µl drops on a glass slide to be desiccated overnight to dryness at 4°C. In the morning, 20 µl of water was used to hydrate the dried proteoliposomes. After >2 h of incubation in a hydrating chamber, proteoliposomes were visible under the microscope and used for patching experiments for that day. The final reconstituted protein/lipid ratios (wt/wt) ranged between ∼1:300 and 1:2,000. This two-step reconstitution procedure consistently generated a large fraction (>50%) of patches with multiple- (1:∼300 ratio) or single-channel (1:1,000 to 2,000) activity.

Protein Analysis

Purified KvLm FL and PM were separated on 12% SDS-PAGE (Fig. 2). Elution volumes and profiles from diagnostic size-exclusion chromatography purification trials of FL-KvLm and KvLm-PM indicated that the channels elute from the affinity column as a homogeneous population of tetramers (not depicted). Positive identification of purified targets was performed by blot analysis (Santos et al., 2006).

Downloaded from http://rupress.org/jgp/article-pdf/132/6/651/1786737/jgp_200810077.pdf by guest on 09 February 2026

Single-Channel Recordings from Giant Proteoliposomes

Excised patches were used (Gambale and Montal, 1990). Pipette and bath solution contained 200 mM KCl and 5 mM HEPES titrated to pH 7.2 with KOH unless otherwise noted. For selectivity measurements, chloride salts of K^+, Na^+, Cs^+, and Rb^+ at 200 mM replaced KCl in the bath solution. Complete exchange of bath solution was accomplished by washing chamber by gravity flow with 10 chamber volumes of new solution. Capillaries of borosilicate glass from both Sutter Instrument Co. and World Precision Instruments were pulled to yield resistances of 5–15 MΩ when immersed in recording solution. Records were acquired at a sampling frequency of >10 kHz and filtered online to 5 kHz with a three-pole Bessel filter before digitization. For all records, the holding voltage was 0 mV and the interpulse interval was >30 s.

Single-Channel Analysis

Data were analyzed using Clampfit v.9.2 software (MDS Analytical Technologies), Excel 2007 (Microsoft), and IGOR Pro (WaveMetrics). Single-channel conductance (γ) was calculated from Gaussian fits to currents histograms. Probability density analysis provides the number of open and closed states and the channel open (τ_o) and closed (τ_c) lifetimes. The voltage dependence of channel opening was calculated from measurements of the fraction of time that the channel is open (P_o) as a function of voltage, either by integration of conductance histograms or from dwell time histograms according to: $P_o = N\tau_o/T$, where N is the number of openings, τ_o is the mean open time, and T is the total recording time at a given voltage (Labarca et al., 1985; Keller et al., 1986). Openings to subconductance states were not included in calculations of P_o. All statistical values represent mean ± SEM, unless otherwise indicated. n and N denote number of experiments and number of events, respectively.

The goal for the analysis of substates was only to catalog the observed conductances. For the analysis of substates, records were filtered to 2 kHz. Transition levels for the detection of events were set only to current levels corresponding to full channel closing and opening, with the exception for records at 200 mV for which an additional level located between closed and open was added. Transitions were identified in Clampfit using the implemented threshold-crossing analysis method where in current deflections that reach one-half of the full transition are included for analysis. Transitions shorter than 0.1 ms were ignored. Transitions from more than five experiments were combined to generate a current histogram for each potential assayed. Substate conductance levels were determined from a least-squares fit of a mixture of multi-Gaussian functions to the current histograms in IGOR (WaveMetrics). The identification of a peak by fit was always cross-checked against the trace. The error for each subconductance determined from current histograms at 150, 180, and 200 mV was calculated by error propagation using one-half of the full width of the fitted Gaussian peaks at half-height as the associated error with each level. For substate analysis of traces in 200 mM KCl, the identified subconductance levels determined at these potentials were pooled and binned according to size and the average values presented ± standard deviation.

Online Supplemental Material

To gain insight into module conservation in Kv channels, the extent of sequence identity between every two sequences in an alignment of 85 FL sequences of candidate bacterial Kvs with the sequences of KvAP and KvLm was calculated (Fig. S1) for the VSM (A, S1-S4), PM including S4-S5 linker (B, PM:S4-S5L-S5-P-S6), and FL without N and C termini (C). The results of this pairwise sequence identity comparison for each module are plotted in a matrix in which each matrix element, corresponding to a sequence identity value between two sequences in the alignment, is color coded: 0–25% identity in white, 25–50% in light gray, 50–75% in dark gray, and 75–100% in black. This representation indicates that the number of light gray and black matrix elements is significantly higher for the PM, implying that the PM sequence in Kv channels is more conserved than the VSM sequence, and that the voltage sensor contributes strongly to Kv channel diversity. Fig. S1 is available at http://www.jgp.org/cgi/content/full/jgp.200810077/DC1.

RESULTS

Recombinant FL-KvLm and Its Pore Assemble as Tetramers

The segregation between voltage sensor and pore observed in the crystal structures of wild-type and chimeric Kv 1.2 (Long et al., 2005a; Long et al., 2007) suggests that in eukaryotic Kv channels, sensor and pore may fold independently. Because sequence alignments of Kv channels of prokaryotic and eukaryotic origin exhibit marked sequence conservation (Santos et al., 2006), we queried whether in prokaryotic Kv channels the pore could fold in the absence of the sensor. Analysis of an alignment of a large number of prokaryotic Kv channel sequences shows that the pores of all prokaryotic Kv channels are remarkably alike (Fig. S1), approaching universality as sequence homology in the selectivity filter and S6 come near identity (Fig. 1, A and B). Fig. 2 shows a Coomassie-stained SDS PAGE of purified FL-KvLm (lane 2) and purified KvLm-PM (lane 3) used for reconstitution. Both proteins migrate close to a molecular mass corresponding to a tetramer: FL-KvLm, 119 kD, and KvLm-PM, 73 kD, indicating that the oligomers are stable and resistant to SDS at room temperature. We conjecture that correct oligomerization is mediated by the correct folding of the pore subunits, an assumption to be validated by the ensuing functional characterization of the pore. The reported successful chimeric coupling between voltage sensors and potassium-selective

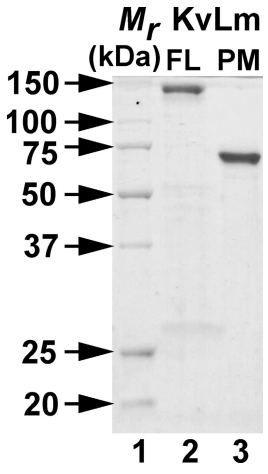

Figure 2. Purification of FL-KvLm and KvLm-PM. Coomassie-stained SDS PAGE: (Lane 1) *Mr* standards. (Lane 2) Purified FL-KvLm. (Lane 3) Purified KvLm-PM used for reconstitution. Both proteins migrate close to a molecular mass corresponding to a tetramer: FL-KvLm, 119 kD, and KvLm-PM, 73 kD.

Downloaded from http://rupress.org/jgp/article-pdf/132/6/651/1786737/jgp_200810077.pdf by guest on 09 February 2026

pores and the structural characterization of the voltage sensor from KvAP (Jiang et al., 2003; Chakrapani et al., 2008) allow us to predict that independent module folding may be a general trademark of voltage-gated channels (Fig. 1 B).

FL-KvLm Gates and Conducts with the Same Properties When Reconstituted in Liposomes or Heterologously Expressed in *E. coli* Spheroplasts

The purified FL-KvLm after reconstitution in giant asolectin proteoliposomes is a voltage-gated, outward rectifier K^+-selective channel. Currents were recorded in symmetric 0.2 M KCl and 5 mM HEPES, pH 7.2. Fig. 3 A displays a current record in response to continuously cycled voltages of −150 to +150 mV. Notably, channel activity appears preponderantly at positive voltages. Note a single opening at around −140 mV of the same conductance as that elicited by the corresponding positive voltage (V), yet with a distinctly lower open probability (P_o). This most likely reflects opening of a single channel inserted in the membrane in the opposite orientation. Fig. 3 B shows segments of a record obtained at a constant negative V of −80, −100, and −120 mV and the corresponding positive V; discrete channel openings are clearly discerned only at positive V with a $\gamma = 45 \pm 2$ pS. These results are comparable to those obtained for FL-KvLm expressed in spheroplast (Santos et al., 2006) for which it was determined that the FL-KvLm is a depolarization-activated channel, therefore suggesting that the orientation of the reconstituted FL-KvLm is predominantly "inside-out."

Sensor Removal Ablates Voltage Dependence and Absolute Rectification

The purified KvLm-PM forms channels with characteristic single-channel conductance and rudimentary voltage-dependent gating properties dictated by the polarity of the transmembrane potential. KvLm-PM channels were reconstituted at low protein to lipid molar ratio (LP ∼1:300), and currents were recorded in symmetrical 200 mM KCl and 5 mM HEPES, pH 7.2. This is shown in Fig. 4. Current recordings under voltage clamp were

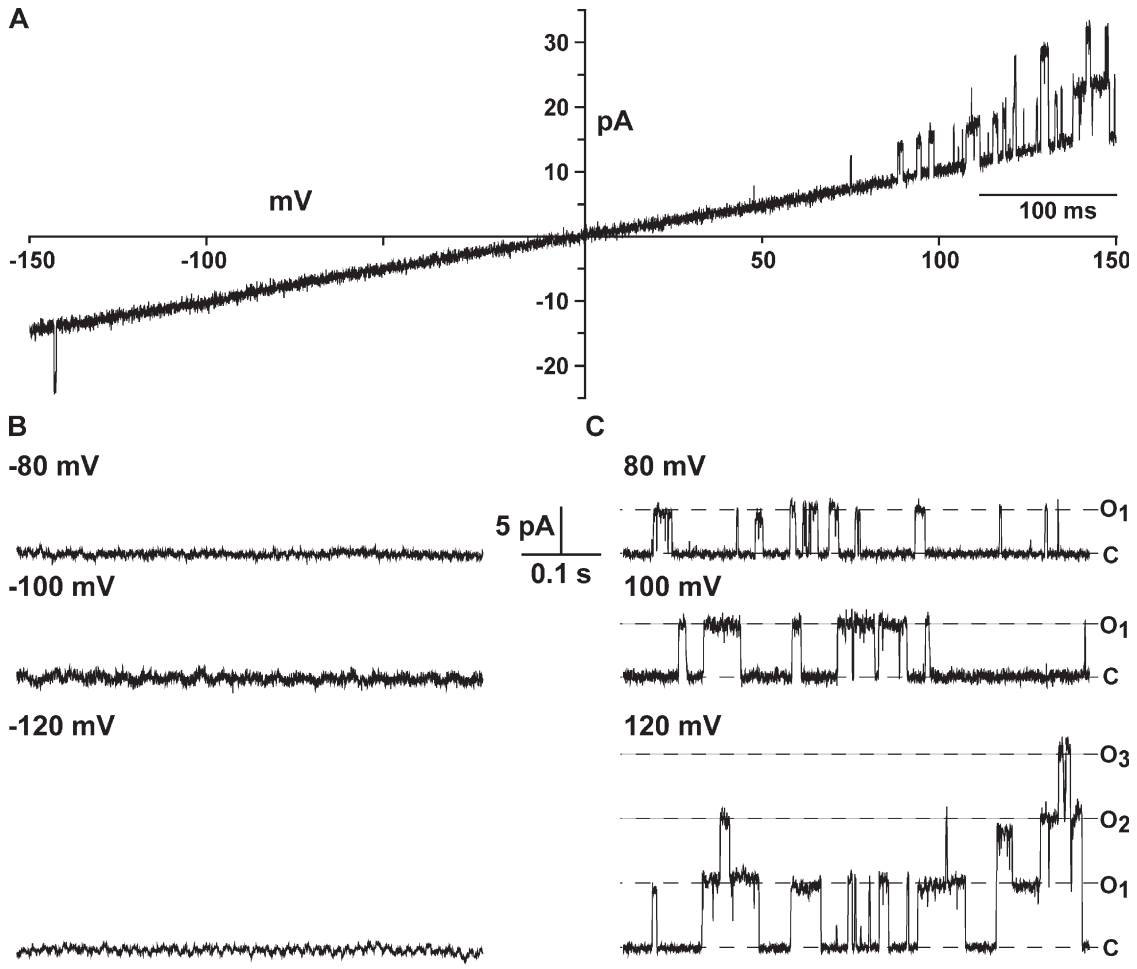

Figure 3. The reconstituted FL-KvLm channel is voltage gated and rectifies strongly. Currents under voltage clamp of reconstituted FL-KvLm channels in asolectin liposomes evoked by a voltage ramp (A) or at constant negative (B) and positive (C) potentials of 80, 100, and 120 mV. Currents were recorded in symmetrical 200 mM KCl and 5 mM HEPES, pH 7.2.

Downloaded from http://rupress.org/jgp/article-pdf/132/6/651/1786737/jgp_200810077.pdf by guest on 09 February 2026

elicited by a voltage ramp (Fig. 4 A) or at constant negative (B) and positive (C) potentials of 50 and 100 mV. These results are remarkable in several ways: (1) They clearly demonstrate that the PM opens in the absence of the sensor module, suggesting that a primary function of the sensor module is to keep the channel closed, a "gatekeeper" as referred to by Armstrong (2003). (2) Inspection of the ramps shown for FL-KvLm in Fig. 3 with that of the isolated PM (Fig. 4) shows that the residence time in the open state is much longer for

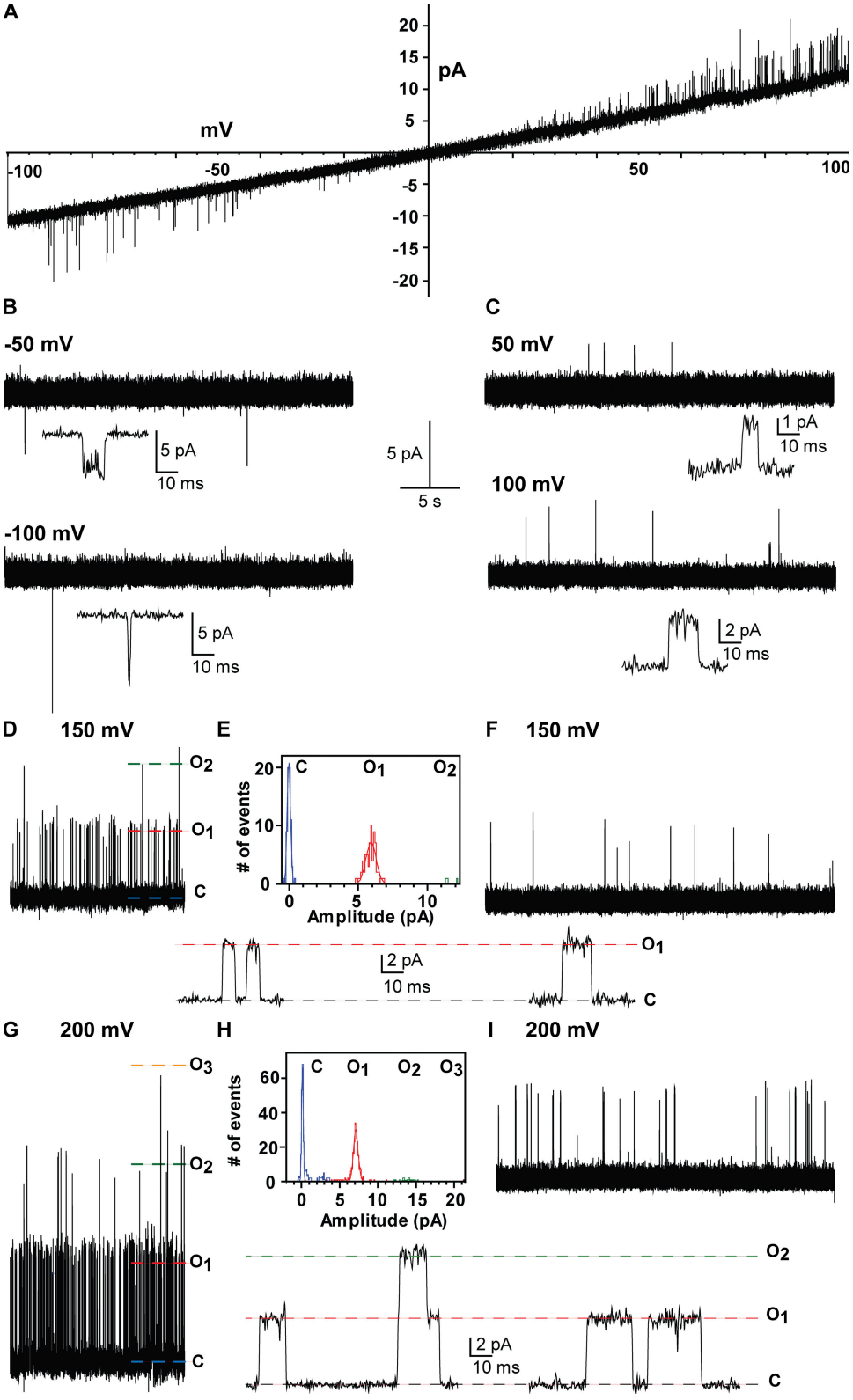

Figure 4. KvLm-PM forms channels with characteristic single-channel conductance and vestigial voltage-dependent gating properties dictated by the polarity of the membrane polarization. KvLm-PM channels were reconstituted at low protein to lipid molar ratio, and currents were recorded in symmetrical 200 mM KCl and 5 mM HEPES, pH 7.2. Current recordings under voltage clamp elicited by a voltage ramp (A) or at constant negative (B) and positive (C) potentials of 50 and 100 mV. Comparison of single channel activity at 150 and 200 mV between patches with high (HP) and low (LP) protein to lipid molar ratio: (D–I) recording at 150 mV and corresponding all-point single-channel current histogram at HP ratio (D and E) and a recording at 150 mV at LP ratio (F); recording at 200 mV and corresponding all-point single-channel current histogram at HP ratio (G and H) and a recording at 200 mV at LP ratio (I). Time expansions of recordings at each potential showing few representative transitions between open and closed are provided below each record.

Downloaded from http://rupress.org/jgp/article-pdf/132/6/651/1786737/jgp_200810077.pdf by guest on 09 February 2026

FL-KvLm than for the PM. This is not a rigorous statement, as we cannot ascertain the number of channels in each patch. (3) The PM exhibits modest rectification insofar as the channels open with a significantly lower probability at negative than at positive voltages, yet is conductive in both directions. Presumably, the PM is tuned to conduct in a preferential direction to match sensor activation. (4) The PM is oriented inside out given that for the positive branch of the voltage ramps the 43 ± 2 pS single-channel chord conductance of PM matches the 45 ± 2 pS of FL-KvLm (Figs. 3 and 5). (5) The PM displays a very low open probability therefore precluding an accurate determination of the number of channels in a given patch. This is shown in Fig. 4 (D–I), which displays a comparison of single-channel activity at 150 and 200 mV between patches with high (HP) and low (LP) protein to lipid molar ratios: recording at 150 mV and corresponding all-point single-channel current histogram at HP ratio (D and E) and a recording at 150 mV at LP ratio (F); and recording at 200 mV and corresponding all-point single-channel current histogram at HP ratio (G and H) and a recording at 200 mV at LP ratio (I). Time expansions of recordings at each potential showing few representative discrete transitions between open and closed are provided below each record; γ = 41 ± 2 pS at 150 mV and 37 ± 2 pS at 200 mV . Clearly, the open probability with three simultaneous open channels is similar to that with one open channel. Therefore, our comparative analysis with FL-KvLm is restricted to current voltage and NP_o relationships (see Fig. 5). (6) The PM does not appear to undergo a time- or voltage-dependent loss of activity, therefore any inactivation in FL-KvLm must necessarily arise from a conformation of the PM imparted by the sensor. (7) Reconstitution at high protein to lipid ratios augments channel density in the patch. Furthermore, the channel properties are indistinguishable regardless of whether the channel was reconstituted at a low or high protein to lipid ratio; evidently, the records obtained at low ratios are authentic.

The reconstituted KvLm-PM retains the single-channel conductance features of FL-KvLm but not the voltage-dependent asymmetry. This is illustrated in Fig. 5. Single channel current–voltage (I-V) relationships in symmetric 0.2 M KCl for FL-KvLm (Fig. 5, filled square; n = 5) and KvLm-PM (open circle; n = 7) are shown in panel A, and the voltage dependence of channel opening for FL-KvLm (filled squares) and KvLm-PM (open circle) are shown in panel B. At depolarizing potentials, the single-channel *I-V* curve is ohmic from 0 to 150 mV with a slope conductance of 43 ± 2 pS, as calculated from single-channel current amplitude histograms (Keller et al., 1986); γ of the isolated PM and of the FL-KvLm are, therefore, indistinguishable. This result in and of itself indicates that the PM oligomerizes within the membrane to a native state. When the isolated PM is reconstituted in liposomes under conditions equivalent to those used in our spheroplast study, which included 40 mM $MgCl_2$ (Lundby et al., 2006; Santos et al., 2006), γ is attenuated to ~16 pS (not depicted) in fair agreement to 18 pS displayed in spheroplasts. The *I-V* plot (Fig. 5 A) and the NP_o-V plot (B) show no data on the negative branch for FL-KvLm, in accord with its voltage-dependent asymmetry (see Fig. 3). For the reconstituted PM, currents are measurable at negative voltages (Fig. 5 A), yet the open probability is virtually null (Fig. 5 B). The single-channel conductance of KvLm-PM is asymmetrical: at −100 mV it is 80 ± 10 pS, ~2.0 times larger than at +100 mV, in agreement with the γ asymmetry observed in single-channel recordings of *Shaker* in symmetrical condition (Heginbotham and MacKinnon, 1993). This directional asymmetry in single-channel conductance could arise from the asymmetrical charge distribution between the outer and inner mouths of the channel, regions in which single mutations that add or remove a formal charge have a large impact on γ

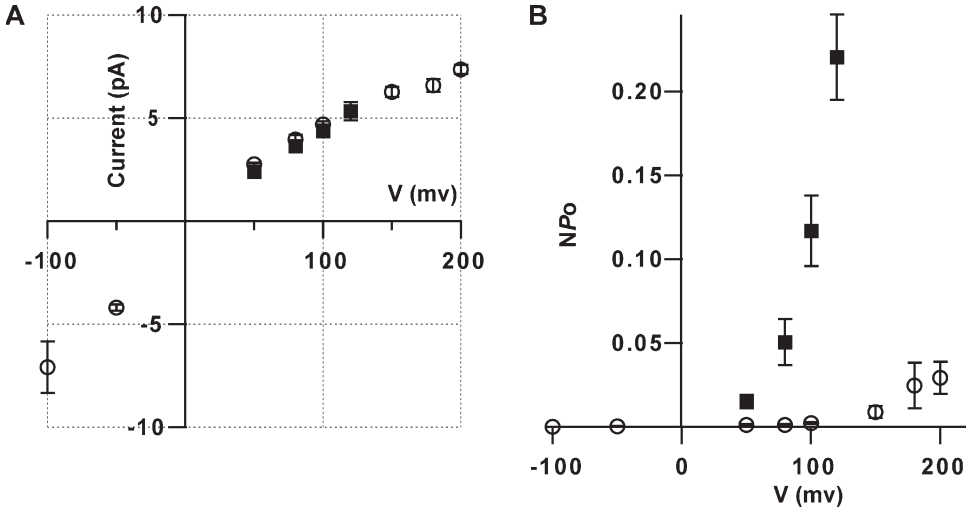

Figure 5. The KvLm-PM retains the single-channel conductance but not the voltage dependence of the FL-KvLm at depolarizing membrane potentials. (A) Single-channel I-V relationships in 200 mM of symmetric KCl for FL-KvLm (filled square; n = 5) and KvLm-PM (open circle; n = 7). (B) Voltage dependence channel opening for FL-KvLm (filled squares) and KvLm-PM (open circle). All values plotted ± SEM.

Downloaded from http://rupress.org/jgp/article-pdf/132/6/651/1786737/jgp_200810077.pdf by guest on 09 February 2026

(Nimigean et al., 2003). Alternatively, the asymmetry could emerge from non-energetically equivalent conduction paths through the filter due to the graded affinity of different binding sites within the filter for the ion (Berneche and Roux, 2005), a feature which appears to be of significance for numerous Kv pores. The NP_o-V plot (Fig. 5 B) shows that at 100 mV, the PM is 60-fold less likely to be in a conducting conformation than the FL (NP_o PM = 0.002, NP_o FL = 0.12). Therefore, the intrinsic voltage dependence of the isolated PM is drastically modulated when in the context of the FL channel given that the FL-KvLm does not show saturation (Fig. 5 B), even at the highest voltage assayed (V = 120 mV). This is in accord with our results on spheroplasts for which the $V_{1/2}$, the voltage at which half of the channels are open, is 152 mV (Lundby et al., 2006; Santos et al., 2006).

KvLm-PM Is Exquisitely Cation Selective

The reconstituted KvLm-PM displays exquisite selectivity for K^+ as shown in the detailed analysis provided in Fig. 6. Fig. 6 A displays currents under voltage clamp from excised membrane patches of the KvLm-PM reconstituted at HP ratio in asolectin proteoliposomes

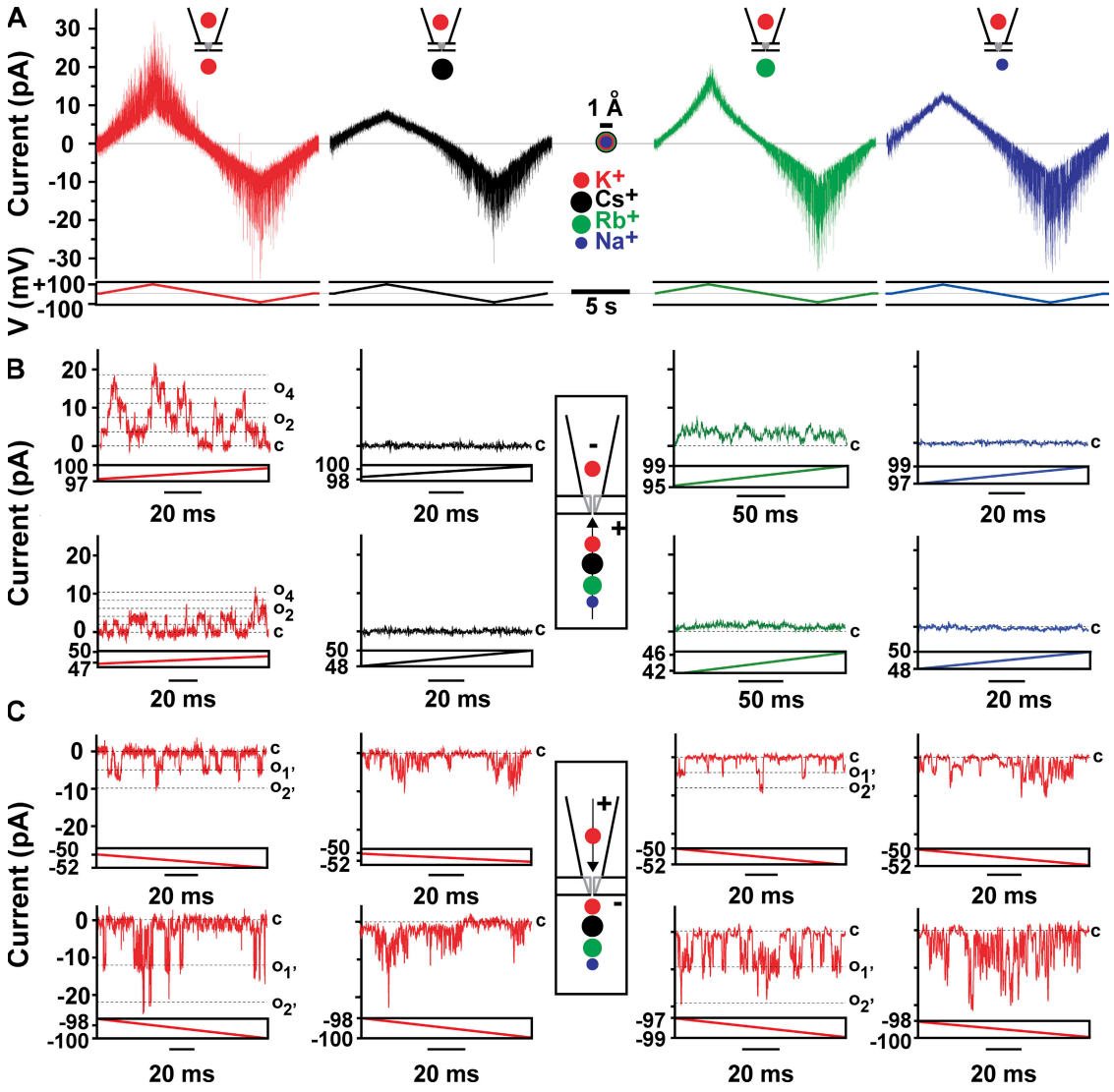

Figure 6. The KvLm-PM is exquisitely selective for K^+. (A) Currents under voltage clamp of the KvLm-PM reconstituted at HP ratio in asolectin liposomes evoked by a voltage ramp recorded in symmetrical 200 mM chloride salt of K^+ (red), or with 200 mM K^+ on pipette and 200 mM Cs^+ (black), Rb^+ (green), and Na^+ (blue) in bath. Traces were recorded successively from a single experiment in the order presented. (B and C) 100- or 250-msec time expansions taken from the ramps shown above at depolarizing (B) and hyperpolarizing (C) membrane potentials. Segments and boundaries of the voltage ramp are depicted in the box under the corresponding current recording. Currents carried by ion in pipette (K^+) are shown in red. Currents carried by ion in bath are shown according to the ramp color scheme. Current levels are shown and labeled whenever clear transitions of uniform conductance could be measured: for symmetric K^+ in both membrane polarities and in asymmetrical K^+/Rb^+ at hyperpolarizing membrane potentials. The ionic radius shown for each cation is the Pauli ionic radius.

Downloaded from http://rupress.org/jgp/article-pdf/132/6/651/1786737/jgp_200810077.pdf by guest on 09 February 2026

evoked by a voltage ramp and recorded in symmetric 0.2-M chloride salts of K^+ (red), or with 200 mM K^+ inside the pipette and 200 mM Cs^+ (black), Rb^+ (green), and Na^+ (blue) in the bath. Traces were recorded successively from a single experiment in the order presented. 100- or 250-msec time expansions taken from the ramps shown above at depolarizing and hyperpolarizing membrane potentials are displayed in Fig. 6 (B and C). Segments and boundaries of the voltage ramp are depicted in the box under the corresponding current recording. Currents carried by the ion in the pipette (K^+) are shown in red. Currents carried by the ion in the bath are depicted according to the ramp color scheme. Current levels are shown and labeled whenever clear transitions of uniform conductance could be measured, namely for symmetric K^+ in both membrane polarities and for asymmetrical K^+/Rb^+ at hyperpolarizing membrane potentials. The ionic radius shown for each cation is the Pauli ionic radius.

The PM channel is highly permeable to K^+, marginally permeable to Rb^+, and impermeable to Na^+ and Cs^+ (Fig. 6, A and B), in agreement with results from FL-KvLm recorded in patches excised from spheroplasts (Lundby et al., 2006; Santos et al., 2006). Under hyperpolarizing voltages, the PM channel appears blocked when a K^+ current is driven against Na^+ or Cs^+, but not against Rb^+ or K^+ (Fig. 6 C); note the short-lived, flickering, and inhomogeneous transitions, all features characteristic of channel block (Hille, 2001). This result suggests that Na^+ and Cs^+ access the filter region and bind there with different affinity. Alternatively, or simultaneously, the preceding depolarizing pulse that loads the cavity with Na^+ or Cs^+ could deplete the filter of K^+ without replenishing it with Na^+, thereby inducing a conformational change in the filter to a nonconductive conformation (Zhou et al., 2001), which is not readily reversible when attempting to reoccupy the ion-binding sites from the extracellular side with K^+. Although we cannot rule out a contribution from either mechanism, the larger decrease in channel conductance when driving K^+ conduction against Cs^+ than against Na^+ highlights a strong contribution from the proposed ion-specific block at the filter. In accordance, conduction in symmetric K^+ in the hyperpolarization direction is shown to promote channel closures within an open burst, significantly decreasing the apparent mean open time.

The Rb^+ permeability through the KvLm-PM is finite, yet the permeability ratio of Rb^+ to K^+ is extremely low. This is shown in Fig. 7. For this analysis, currents were measured at high ionic strength to increase the signal to noise ratio. Currents were evoked from a holding potential of 0 mV to depolarizing potentials of 100, 150, and 200 mV in symmetric 0.5 M KCl (Fig. 7 A, red) or 0.5 M RbCl (B, green) and 5 HEPES, pH 7.2. For the Rb^+ currents, the sections delimited by the black lines are displayed at a higher gain above the corresponding records. These recordings were obtained from preparations generated from the same purification batch and reconstituted at the same protein to lipid ratio. Of note is the significantly longer mean open time in Rb^+ than in K^+, consistent with a longer residence time of Rb^+ in the filter region. This is a remarkable result insofar as the reconstituted PM recapitulates the prolonged residence time in the open state when the selectivity filter is occupied by Rb^+, a feature known to occur in *Shaker* Kv channels (Swenson and Armstrong, 1981). The single-channel I-V relationships and the voltage-dependence of channel opening in symmetric 0.5 M KCl (Fig. 7, red bar; $n = 5$) and RbCl (green bar; $n = 5$) for KvLm-PM are displayed in panels C and D. All values plotted ± SEM. γ is approximately twofold higher in symmetric 0.5 M KCl

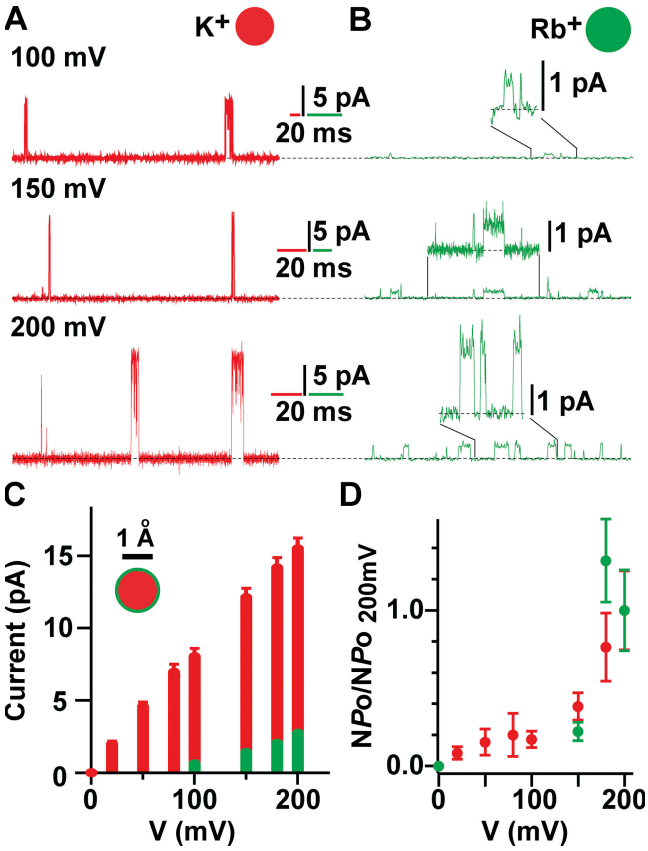

Figure 7. The Rb^+ permeability through the KvLm-PM is finite, yet the permeability ratio of Rb^+ to K^+ is extremely low. Currents evoked from a holding potential of 0 mV to depolarizing potentials of 100, 150, and 200 mV in symmetrical 0.5 M KCl (A, red) or 0.5 M RbCl (B, green) and 5 HEPES, pH 7.2. For the Rb^+ currents, the sections delimited by the black lines are displayed at a higher gain above the corresponding records. Currents traces in 0.5 M KCl were filtered to 2 kHz, whereas those in 0.5M Rb were filtered to 500 Hz. (C) Single-channel I-V relationships in symmetric 0.5 M KCl (red bar; $n = 5$) and RbCl (green bar; $n = 5$) for KvLm PM. Normalized voltage dependence of KvLm-PM opening in 0.5 M KCl (red) and RbCl (green). All values plotted ± SEM.

Downloaded from http://rupress.org/jgp/article-pdf/132/6/651/1786737/jgp_200810077.pdf by guest on 09 February 2026

than in 0.2 M KCl (Fig. 5). The Rb^+/K^+ conductance ratio is ≤0.16. Thus, the voltage dependence of KvLm-PM opening appears unaltered by high ionic strength, validating the fidelity of the results.

Tetrabutylammonium (TBA) Blocks Currents in KvLm-PM and FL-KvLm with High Affinity

The results summarized thus far strongly support the view that the PM is sufficient to recapitulate the conduction and permeability features that are characteristic of the FL channel. How about channel blocking? As shown in Fig. 8, TBA blocks both the FL-KvLm channel and its isolated PM with high affinity. Fig. 8 A displays TBA blocking of KvLm-PM single-channel currents at the indicated TBA concentration; TBA was supplemented only to the bath compartment, presumed to be cytoplasm. The records are displayed at slow-time resolution to convey the time course and extent of block. Three channels are present that exhibit a progressively smaller conductance and a bursting pattern of channel activity, which arises from transitions between open and blocked states. The fast flicker of channel current combined with a reduced γ are hallmark features of channel block (Hille, 2001). These results for KvLm-PM are in accord with the results for FL-KvLm (Lundby et al., 2006; Santos et al., 2006). Fig. 8 B shows the fraction of blocked FL-KvLm (filled squares) and KvLm-PM (open circles) channels at micromolar concentrations of TBA; membrane potential was held at 100 mV. The best fit to the data with "Fraction of blocked channels = $1/(1 + K_d/[TBA])$" is shown with K_d values of 0.36 ± 0.01 μM for FL-KvLm and 27 ± 2 μM for KvLm-PM.

Thus, TBA blocks the isolated PM with μM affinity, and the FL-KvLm with nM affinity in agreement with our previous study on membrane patches from bacterial spheroplasts (Lundby et al., 2006; Santos et al., 2006), and with a plethora of studies from several members of the Kv channel family (Armstrong and Hille, 1998). The implication of these results is that the tertiary structure of the PM in isolation, as an independent entity, or when integrated with the sensor in the context of di-modular KvLm channel is similar. Given that TBA block of K^+-selective channels requires the channel to open (French and Shoukimas, 1981; Liu et al., 1997; Faraldo-Gomez et al., 2007; Yohannan et al., 2007) it is likely that the notable difference in K_d between PM and FL reflects the low open probability of the KvLm-PM.

Sensor Clipping Discloses Subconductance States

In current recordings with a high channel density, KvLm-PM opens to conduct current a fraction of the size of the whole single channel current (Fig. 9, B, C, and E, S1 and S2). To characterize these subconductance states, all-point current histograms from five traces recorded at 150, 180, and 200 mV were combined and fit with multi-peak Gaussian (Fig. 9, A, D, and F). This analysis clearly identified the presence of at least two subconductance states: S1 with an average γ of 15 ± 4 pS (37 ± 9% of the open γ), and S2 with an average γ of 32 ± 3 pS (78 ± 7% of the open γ) (see Fig. 9 G). Time-expanded current traces at 150 and 180 mV (Fig. 9, C and E) show that residency in either state need not be en route to full channel opening; this is especially clear for S1, a substate in which the channel can dwell for milliseconds before closing. In contrast to visits to S2 that appear to occur with equal frequency in the voltage range tested, visits to S1 are seen to occur more frequently at potentials below 200 mV, the membrane potential at which P_o for the KvLm-PM is highest (Fig. 5 B). Also, unlike residency in S1, residency in the S2 sublevel has been observed consistently to be of very short duration and could therefore be attributed to transitions within open-channel noise or incomplete captures of the full transition limited by the resolution of the recording. Admittedly, the current trace evoked from a pulse to 150 mV displays several long-lasting transitions to a current level that is ∼40%

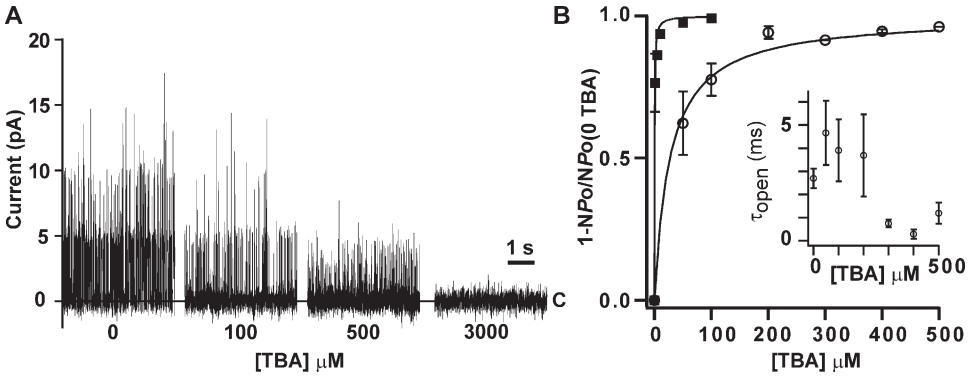

Figure 8. TBA blocks FL-KvLm and KvLm-PM with high affinity. (A) TBA blocking of KvLm-PM single-channel currents at the indicated TBA concentration. (B) Fraction of blocked FL-KvLm (filled squares) and KvLm-PM (open circles) channels at micromolar concentrations of TBA. The best fit to the data with "Fraction of blocked channels = $1/(1 + K_d/[TBA])$" is shown with K_d values of 0.36 ± 0.01 mM for FL-KvLm and 27 ± 2 mM for KvLm-PM. Inset shows the dependency of the mean open time of the KvLm-PM first open channel at each TBA concentration. Because the number of channels in each patch cannot be accurately determined, this plot is intended to provide only an overview. Membrane potential was 100 mV. All values are reported with ± SEM.

Downloaded from http://rupress.org/jgp/article-pdf/132/6/651/1786737/jgp_200810077.pdf by guest on 09 February 2026

of S1, which we shall call S0. The best fit to the sum histogram clearly did not have a Gaussian peak at this current level; therefore, we surmise that we were not able to collect enough transitions to this level from the five experiments pooled. The agreement between percent γ of KvLm-PM substates and substates recorded in eukaryotic Kv channels suggests a common origin for the substate: conduction through channel oligomers in which less than four subunits are activated (Hoshi et al., 1994; Chapman et al., 1997; Zheng and Sigworth, 1997, 1998; Zheng et al., 2001; Chapman and VanDongen, 2005). Therefore, we tentatively assign S0, S1, and S2 substates to conduction through oligomers with one, two, or three subunits in the conductive conformation. This interpretation, over for example a substate originating from different size oligomers or conduction through intra-subunit pathways, is justified by three additional lines of evidence: (1) the KvLm-PM population of channels reconstituted is observed to be homogeneously tetrameric by size-exclusion chromatography and by SDS-PAGE in the presence of asolectin (unpublished data); (2) replacement of NaCl by KCl

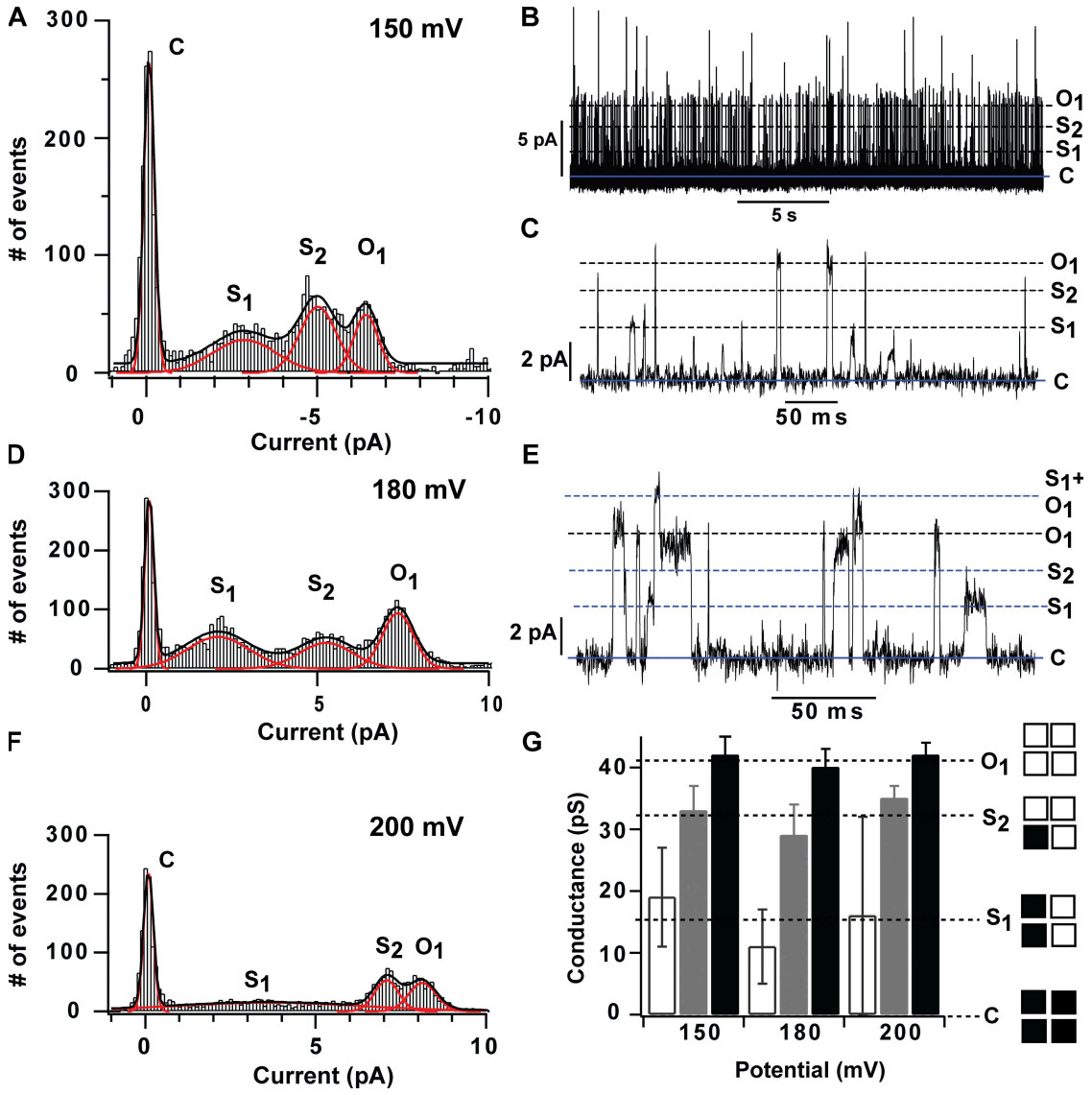

Figure 9. The KvLm-PM exhibits two subconductance levels that are populated with decreasing frequency as the applied potential is increased. Single-channel current histograms (A, D, and F) were accumulated from recordings at 150, 180, and 200 mV on five patches from five different reconstitution events. Two of the traces recorded at 150 and 180 mV showing the presence of substates are presented in B, C, and E. The transition threshold levels for identifying a transition between levels were set so as to pick up the most number of transitions without artificially enhancing noise. The records were digitized at 10 kHz and filtered to 2 kHz for display (B, C, and E) and analysis. The conductance of the sublevels was determined from Gaussian fits to the all-point current histogram and displayed in bar graph format (no fill, S1; gray fill, S2; black fill, Open) at each test potential in G. A total of 3,855, 5,246, and 3,153 events from recordings at 150, 180, and 200 mV were analyzed.

Downloaded from http://rupress.org/jgp/article-pdf/132/6/651/1786737/jgp_200810077.pdf by guest on 09 February 2026

in growth media is highly toxic to bacteria expressing KvLm-PM but not FL-KvLm; and (3) the conductance of each substate varies nonlinearly with the number of predicted subunits in the conductive form. The observation of conduction substates with high frequency in KvLm-PM but not in FL-KvLm suggests that in the absence of the sensor, cooperativity in pore opening—seen in the concerted activation of all four channel subunits into a single conductive conformation in FL-KvLm—is affected, especially at potentials below 200 mV, but clearly not abolished. It is surmised that the concerted opening of the pore in FL-KvLm is in part attributed to a property of the pore alone.

DISCUSSION

Identification of Two Gates in the KvLm PM

An important inference from the results presented here is that the KvLm-PM can activate on its own, suggesting that the open and closed conformations of the pore exist in close energetic equilibrium. Evidence that Na^+ and Cs^+ can be loaded onto the internal cavity of the channel (see Fig. 6 C) only to be removed by forcing K^+ to pass in the opposite direction evoking a conduction phenotype that resembles that of a blocked channel strongly supports the conclusion that a failure to conduct Na^+ or Cs^+ by the KvLm-PM is not due to the inaccessibility of these ions to the inside of the channel. Likewise, the ability to block the channel with TBA, an open-channel blocker (French and Shoukimas, 1981; Liu et al., 1997; Faraldo-Gomez et al., 2007; Yohannan et al., 2007), which like other quaternary ammonium compounds (Armstrong, 1971) blocks currents through K^+-selective pores from the intracellular side, shows that the gate of the channel opens wide enough from the cytoplasmic side to let the blocker through. These results validate the view that the gate in the pore of KvLm opens as wide in the sensorless KvLm-PM as in FL-KvLm. Collectively, TBA block and accessibility of Na^+ and Cs^+ to the channel cavity support the postulate that there are two gates in KvLm-PM, one near the cytoplasmic side suggested to arise from the S6 helix bundle crossing (Liu et al., 1997), and the other near the extracellular boundary as proposed for other eukaryotic Kv channels (Armstrong et al., 1982; Miller et al., 1987; Berneche and Roux, 2005). Furthermore, the asymmetry observed in single-channel conductance at every polarity tested strongly suggests that the conduction path between the two gates is not equally favorable in either direction. Conceivably, this arises from non-energetically equivalent paths through the filter region of the channel, in agreement with the apparent decrease in the mean open time when conducting in the hyperpolarizing direction.

Comparison between Subconductance States in KvLm and Other Kv Channels

It is widely recognized that the detection frequency of conduction substates in eukaryotic Kv channels is low (Hoshi et al., 1994; Chapman et al., 1997; Zheng and Sigworth, 1997; Schoppa and Sigworth, 1998a), presumably because residency time is short relative to the acquisition and filtering rates (Zheng and Sigworth, 1998; Shapovalov and Lester, 2004; Chapman and VanDongen, 2005). These surmised invisible transitions are discerned by adding mutations to the sensor (Chapman et al., 1997) or pore (Zheng and Sigworth, 1997, 1998; Zheng et al., 2001), which presumably act by slowing down the final step in channel activation. Alternatively, substates can be drawn out from heteromultimeric assemblies of Kv channel subunits that differ either in the voltage range of activation (Chapman and VanDongen, 2005) or in conductance (Zheng and Sigworth, 1998). In homomultimeric wild-type Kv channels, Hoshi et al. (1994) reported *Shaker* channel openings to 30 and 60% of the full open γ, whereas Chapman et al. (1997) and Chapman and VanDongen (2005) reported subconductance levels of 15, 37, 58, and 82% of the full open drk1 channel γ and rigorously assigned them to heteromeric pore conformations in which one, two (37 and 58%), or three subunits are in the conductive mode. From the analysis of these substates, a subunit activation model was proposed that predicts that the occupancy of subconduction states is limited at potentials at which the open probability of the Kv channel saturates (Chapman and VanDongen, 2005). The observed increased frequency of conduction substates in KvLm-PM at potentials below which the NP_o-V curve is highest in accord with the proposed model, as are the conductances of the substates: S1 is 37 ± 9% and S2 is 78 ± 7% of the full open, all subunits in conductive mode, i.e., 41 ± 2 pS. Although we could not detect enough transitions into a substate with a single subunit in the conductive state (15% of drk1 γ), we did observe in several recordings at 150 mV subconductance states ∼40% of S1 or ∼15% of the single-channel conductance of KvLm-PM (see Fig. 9 C). The striking agreement between model predictions and observed KvLm-PM subunit gating allows a speculative assignment of S1 and S2 to conduction through oligomers with two and three subunits in the conductive conformation. It also argues that conduction through the pore of a sensorless Kv channel is not an all-or-nothing event.

Semblance between PM Gating Transitions and the Last Transition Preceding Kv Channel Opening

The striking similarities between subconductance states in KvLm-PM and in eukaryotic Kv channels, and the remarkable equivalence of the single-channel conduction properties of KvLm-PM and FL-KvLm, are interpreted as an indication that the observed gating transitions in

Downloaded from http://rupress.org/jgp/article-pdf/132/6/651/1786737/jgp_200810077.pdf by guest on 09 February 2026

KvLm-PM manifest the last structural transition in the pore preceding the onset of ion conduction through Kv channels. In KvLm-PM, pore subunits are observed to gate independently with rudimentary voltage dependence. The increased frequency of conduction substates at potentials below which the NP_o-V curve is highest is interpreted as evidence that each subunit is gated independently by the membrane potential. At saturating membrane potentials, the channel appears to open cooperatively because the subunit dependence on V has saturated (see Fig. 5 B). This assertion is validated by the demonstration that selective analysis of transitions between open and closed, excluding transitions to and from subconductance states, shows a marked increase in the channel open probability (Figs. 5 B and 7 D). The drastic decrease in pore opening probability and conservation of concerted pore opening in KvLm-PM suggests that the sensor plays two major roles in KvLm: (1) to keep the channel closed; and (2) when a sensor subunit is activated to act as an allosteric modulator by shifting the equilibrium of the physically attached pore subunit from resting toward activated state, as proposed by Chapman and VanDongen (2005) for the drk1 channel and by Zheng and Sigworth (1998) for the *Shaker* channel. Our results suggest that in eukaryotic Kv channels, the last transition before the start of ion conduction may have a contribution from charge movement within each pore subunit in response to the applied field, as suggested by Zheng and Sigworth for *Shaker* (Zheng et al., 2001). In their gating model, Zheng and Sigworth endorse the hypothesis that this charge movement is correlated with a conformational change at the upper (extracellular facing) gate largely because they find that the *Shaker* mutant studied exhibits nonselective subconduction states. Because in KvLm-PM we find no evidence for loss of selectivity during subconduction, we suggest that even though the upper gate may change conformation in this last step, the charge movement initiating this conformational change may also lie somewhere else, possibly at the S4-S5 linker that is included in the KvLm-PM construct, and is proposed to interact specifically with S6 to mechanically couple sensor activation to pore gating in eukaryotic Kv channels (Lu et al., 2001, 2002; Long et al., 2005b; Pathak et al., 2007). Therefore, the last structural transition in FL-KvLm only appears to be cooperative because each of the four sensors positions the attached pore subunit ready to conduct in close synchrony, but in essence there is little evidence that the shift from activated and nonconductive to activated and conductive state is cooperative. This interpretation argues that Kv channels in which pore subunit activation has been slowed down will exhibit conduction substates and that these substates will differ from those observed in wild-type Kv channels only in their residency time but not in their identity. This indeed has been shown for eukaryotic Kv channels drk1 and *Shaker* and now also for the prokaryotic KvLm.

Concluding Remarks

Our analysis has been guided by the fundamental tenet that voltage-gated channel proteins are modular in design, and that the coupling between the component modules underlies their exquisite sensitivity to voltage. The results reported here support the modular design of Kv channels in terms of the structural and functional independence of voltage sensing and PMs. If the pore of eukaryotic Kv channels is at all like that of KvLm, experiments on a sensorless *Shaker* channel should prove very informative but equally daunting. The expression of the KvLm-PM is toxic at low K^+ concentrations, presumably because *E. coli* is unable to cope with an errant gating K^+-selective pore when the inward driving force is ~100 mV (assuming a resting potential of −200 mV in *E. coli*) (Meury and Kepes, 1981). In support of this interpretation for bacterial toxicity is our inability to express KvLm-PM in TK2420 cells (Buurman et al., 2004), a strain that requires >10 mM KCl in growing media and presumably copes with an ~−300-mV resting potential (Madrid et al., 1998), which also precluded us from assaying KvLm-PM function in spheroplasts. However, because toxicity was specific to K^+ in the growing media—a tribute to the selectivity of the KvLm-PM—and given the unparallel freedom in manipulating bacterial versus eukaryotic cell growth media, such experiments were feasible in *E. coli*. Nonetheless, it was the documented functional and structural modularity of eukaryotic Kv channels that drove the hypothesis behind this study, and yet we unveil in the prokaryotic KvLm-PM subconductance states a similarity to those observed in mutant eukaryotic Kv channels. There are still many lessons on the workings of eukaryotic Kv's to be learned from the characterization of their prokaryotic counterparts.

We thank Alicia Lundby for her valiant effort to record KvLm-PM currents in spheroplasts and the members of M. Montal's group for valuable help and discussions throughout this work.

This work was supported by a grant from the National Institutes of Health (R01-GM49711 to M. Montal).

Part of this work was presented in poster format at the 2007 meetings of the Biophysical Society (Poster no. 1377) and the Portuguese Society of Neurosciences (SPN).

Edward N. Pugh Jr. served as editor.

Submitted: 10 July 2008
Accepted: 10 November 2008

REFERENCES

Aggarwal, S.K., and R. MacKinnon. 1996. Contribution of the S4 segment to gating charge in the Shaker K+ channel. *Neuron.* 16:1169–1177.

Alabi, A.A., M.I. Bahamonde, H.J. Jung, J.I. Kim, and K.J. Swartz. 2007. Portability of paddle motif function and pharmacology in voltage sensors. *Nature.* 450:370–375.

Armstrong, C.M. 1971. Interaction of tetraethylammonium ion derivatives with the potassium channels of giant axons. *J. Gen. Physiol.* 58:413–437.

Downloaded from http://rupress.org/jgp/article-pdf/132/6/651/1786737/jgp_200810077.pdf by guest on 09 February 2026

Armstrong, C.M. 2003. Voltage-gated K channels. *Sci. STKE.* 2003:re10.

Armstrong, C.M., and B. Hille. 1998. Voltage-gated ion channels and electrical excitability. *Neuron.* 20:371–380.

Armstrong, C.M., R.P. Swenson Jr., and S.R. Taylor. 1982. Block of squid axon K channels by internally and externally applied barium ions. *J. Gen. Physiol.* 80:663–682.

Bao, H., A. Hakeem, M. Henteleff, J.G. Starkus, and M.D. Rayner. 1999. Voltage-insensitive gating after charge-neutralizing mutations in the S4 segment of Shaker channels. *J. Gen. Physiol.* 113:139–151.

Berneche, S., and B. Roux. 2005. A gate in the selectivity filter of potassium channels. *Structure.* 13:591–600.

Bezanilla, F. 2002. Voltage sensor movements. *J. Gen. Physiol.* 120:465–473.

Bezanilla, F. 2005. Voltage-gated ion channels. *IEEE Trans. Nanobioscience.* 4:34–48.

Buurman, E.T., D. McLaggan, J. Naprstek, and W. Epstein. 2004. Multiple paths for nonphysiological transport of K+ in Escherichia coli. *J. Bacteriol.* 186:4238–4245.

Cai, S.Q., K.H. Park, and F. Sesti. 2006. An evolutionarily conserved family of accessory subunits of K+ channels. *Cell Biochem. Biophys.* 46:91–99.

Cao, Y., N.M. Crawford, and J.I. Schroeder. 1995. Amino terminus and the first four membrane-spanning segments of the Arabidopsis K+ channel KAT1 confer inward-rectification property of plant-animal chimeric channels. *J. Biol. Chem.* 270:17697–17701.

Caprini, M., S. Ferroni, R. Planells-Cases, J. Rueda, C. Rapisarda, A. Ferrer-Montiel, and M. Montal. 2001. Structural compatibility between the putative voltage sensor of voltage-gated K+ channels and the prokaryotic KcsA channel. *J. Biol. Chem.* 276:21070–21076.

Caprini, M., M. Fava, P. Valente, G. Fernandez-Ballester, C. Rapisarda, S. Ferroni, and A. Ferrer-Montiel. 2005. Molecular compatibility of the channel gate and the N terminus of S5 segment for voltage-gated channel activity. *J. Biol. Chem.* 280:18253–18264.

Chakrapani, S., L.G. Cuello, D.M. Cortes, and E. Perozo. 2008. Structural dynamics of an isolated voltage-sensor domain in a lipid bilayer. *Structure.* 16:398–409.

Chapman, M.L., and A.M. VanDongen. 2005. K channel subconductance levels result from heteromeric pore conformations. *J. Gen. Physiol.* 126:87–103.

Chapman, M.L., H.M. VanDongen, and A.M. VanDongen. 1997. Activation-dependent subconductance levels in the drk1 K channel suggest a subunit basis for ion permeation and gating. *Biophys. J.* 72:708–719.

Clamp, M., J. Cuff, S.M. Searle, and G.J. Barton. 2004. The Jalview Java alignment editor. *Bioinformatics.* 20:426–427.

Cordero-Morales, J.F., L.G. Cuello, and E. Perozo. 2006a. Voltage-dependent gating at the KcsA selectivity filter. *Nat. Struct. Mol. Biol.* 13:319–322.

Cordero-Morales, J.F., L.G. Cuello, Y. Zhao, V. Jogini, D.M. Cortes, B. Roux, and E. Perozo. 2006b. Molecular determinants of gating at the potassium-channel selectivity filter. *Nat. Struct. Mol. Biol.* 13:311–318.

Cordero-Morales, J.F., V. Jogini, A. Lewis, V. Vasquez, D.M. Cortes, B. Roux, and E. Perozo. 2007. Molecular driving forces determining potassium channel slow inactivation. *Nat. Struct. Mol. Biol.* 14:1062–1069.

Cortes, D.M., L.G. Cuello, and E. Perozo. 2001. Molecular architecture of full-length KcsA: role of cytoplasmic domains in ion permeation and activation gating. *J. Gen. Physiol.* 117:165–180.

Cuello, L.G., J.G. Romero, D.M. Cortes, and E. Perozo. 1998. pH-dependent gating in the Streptomyces lividans K+ channel. *Biochemistry.* 37:3229–3236.

Cuello, L.G., D.M. Cortes, and E. Perozo. 2004. Molecular architecture of the KvAP voltage-dependent K+ channel in a lipid bilayer. *Science.* 306:491–495.

Darszon, A., C.A. Vandenberg, M. Schonfeld, M.H. Ellisman, N.C. Spitzer, and M. Montal. 1980. Reassembly of protein-lipid complexes into large bilayer vesicles: perspectives for membrane reconstitution. *Proc. Natl. Acad. Sci. USA.* 77:239–243.

Ding, S., L. Ingleby, C.A. Ahern, and R. Horn. 2005. Investigating the putative glycine hinge in Shaker potassium channel. *J. Gen. Physiol.* 126:213–226.

Eddy, S.R. 1998. Profile hidden Markov models. *Bioinformatics.* 14:755–763.

Epstein, W., and B.S. Kim. 1971. Potassium transport loci in Escherichia coli K-12. *J. Bacteriol.* 108:639–644.

Faraldo-Gomez, J.D., E. Kutluay, V. Jogini, Y. Zhao, L. Heginbotham, and B. Roux. 2007. Mechanism of intracellular block of the KcsA K+ channel by tetrabutylammonium: insights from X-ray crystallography, electrophysiology and replica-exchange molecular dynamics simulations. *J. Mol. Biol.* 365:649–662.

French, R.J., and J.J. Shoukimas. 1981. Blockage of squid axon potassium conductance by internal tetra-N-alkylammonium ions of various sizes. *Biophys. J.* 34:271–291.

Gambale, F., and M. Montal. 1990. Voltage-gated sodium channels expressed in the human cerebellar medulloblastoma cell line TE671. *Brain Res. Mol. Brain Res.* 7:123–129.

Gao, L., X. Mi, V. Paajanen, K. Wang, and Z. Fan. 2005. Activation-coupled inactivation in the bacterial potassium channel KcsA. *Proc. Natl. Acad. Sci. USA.* 102:17630–17635.

Gonnet, G.H., M.A. Cohen, and S.A. Benner. 1992. Exhaustive matching of the entire protein sequence database. *Science.* 256:1443–1445.

Greenblatt, R.E., Y. Blatt, and M. Montal. 1985. The structure of the voltage-sensitive sodium channel. Inferences derived from computer-aided analysis of the Electrophorus electricus channel primary structure. *FEBS Lett.* 193:125–134.

Grigoriev, S.M., C. Muro, L.M. Dejean, M.L. Campo, S. Martinez-Caballero, and K.W. Kinnally. 2004. Electrophysiological approaches to the study of protein translocation in mitochondria. *Int. Rev. Cytol.* 238:227–274.

Hardman, R.M., P.J. Stansfeld, S. Dalibalta, M.J. Sutcliffe, and J.S. Mitcheson. 2007. Activation gating of hERG potassium channels: S6 glycines are not required as gating hinges. *J. Biol. Chem.* 282:31972–31981.

Heginbotham, L., and R. MacKinnon. 1993. Conduction properties of the cloned Shaker K+ channel. *Biophys. J.* 65:2089–2096.

Hille, B. 2001. Ion Channels of Excitable Cells. 3rd Edition. Sinauer, Sunderland, MA. 814 pp.

Hoshi, T., W.N. Zagotta, and R.W. Aldrich. 1994. Shaker potassium channel gating. I: transitions near the open state. *J. Gen. Physiol.* 103:249–278.

Jiang, Y., A. Lee, J. Chen, M. Cadene, B.T. Chait, and R. MacKinnon. 2002a. Crystal structure and mechanism of a calcium-gated potassium channel. *Nature.* 417:515–522.

Jiang, Y., A. Lee, J. Chen, M. Cadene, B.T. Chait, and R. MacKinnon. 2002b. The open pore conformation of potassium channels. *Nature.* 417:523–526.

Jiang, Y., A. Lee, J. Chen, V. Ruta, M. Cadene, B.T. Chait, and R. MacKinnon. 2003. X-ray structure of a voltage-dependent K+ channel. *Nature.* 423:33–41.

Jogini, V., and B. Roux. 2007. Dynamics of the Kv1.2 voltage-gated K+ channel in a membrane environment. *Biophys. J.* 93:3070–3082.

Keller, B.U., R.P. Hartshorne, J.A. Talvenheimo, W.A. Catterall, and M. Montal. 1986. Sodium channels in planar lipid bilayers. Channel gating kinetics of purified sodium channels modified by batrachotoxin. *J. Gen. Physiol.* 88:1–23.

Kuo, A., J.M. Gulbis, J.F. Antcliff, T. Rahman, E.D. Lowe, J. Zimmer, J. Cuthbertson, F.M. Ashcroft, T. Ezaki, and D.A. Doyle. 2003.

Downloaded from http://rupress.org/jgp/article-pdf/132/6/651/1786737/jgp_200810077.pdf by guest on 09 February 2026

Crystal structure of the potassium channel KirBac1.1 in the closed state. *Science.* 300:1922–1926.

Kuo, M.M., W.J. Haynes, S.H. Loukin, C. Kung, and Y. Saimi. 2005. Prokaryotic K(+) channels: from crystal structures to diversity. *FEMS Microbiol. Rev.* 29:961–985.

Kuo, M.M., K.A. Baker, L. Wong, and S. Choe. 2007. Dynamic oligomeric conversions of the cytoplasmic RCK domains mediate MthK potassium channel activity. *Proc. Natl. Acad. Sci. USA.* 104:2151–2156.

Labarca, P., J.A. Rice, D.R. Fredkin, and M. Montal. 1985. Kinetic analysis of channel gating. Application to the cholinergic receptor channel and the chloride channel from Torpedo californica. *Biophys. J.* 47:469–478.

Ledwell, J.L., and R.W. Aldrich. 1999. Mutations in the S4 region isolate the final voltage-dependent cooperative step in potassium channel activation. *J. Gen. Physiol.* 113:389–414.

Liu, Y., M. Holmgren, M.E. Jurman, and G. Yellen. 1997. Gated access to the pore of a voltage-dependent K+ channel. *Neuron.* 19:175–184.

Long, S.B., E.B. Campbell, and R. Mackinnon. 2005a. Crystal structure of a mammalian voltage-dependent Shaker family K+ channel. *Science.* 309:897–903.

Long, S.B., E.B. Campbell, and R. Mackinnon. 2005b. Voltage sensor of Kv1.2: structural basis of electromechanical coupling. *Science.* 309:903–908.

Long, S.B., X. Tao, E.B. Campbell, and R. MacKinnon. 2007. Atomic structure of a voltage-dependent K+ channel in a lipid membrane-like environment. *Nature.* 450:376–382.

Lu, Z., A.M. Klem, and Y. Ramu. 2001. Ion conduction pore is conserved among potassium channels. *Nature.* 413:809–813.

Lu, Z., A.M. Klem, and Y. Ramu. 2002. Coupling between voltage sensors and activation gate in voltage-gated K^+ channels. *J. Gen. Physiol.* 120:663–676.

Lundby, A., J.S. Santos, C. Zazueta, and M. Montal. 2006. Molecular template for a voltage sensor in a novel K^+ channel. II. Conservation of a eukaryotic sensor fold in a prokaryotic K^+ channel. *J. Gen. Physiol.* 128:293–300.

MacKinnon, R. 1991. Determination of the subunit stoichiometry of a voltage-activated potassium channel. *Nature.* 350:232–235.

Madrid, R., M.J. Gomez, J. Ramos, and A. Rodriguez-Navarro. 1998. Ectopic potassium uptake in trk1 trk2 mutants of Saccharomyces cerevisiae correlates with a highly hyperpolarized membrane potential. *J. Biol. Chem.* 273:14838–14844.

Magidovich, E., and O. Yifrach. 2004. Conserved gating hinge in ligand- and voltage-dependent K+ channels. *Biochemistry.* 43:13242–13247.

Meury, J., and A. Kepes. 1981. The regulation of potassium fluxes for the adjustment and maintenance of potassium levels in Escherichia coli. *Eur. J. Biochem.* 119:165–170.

Miller, C., R. Latorre, and I. Reisin. 1987. Coupling of voltage-dependent gating and Ba^{++} block in the high-conductance, Ca^{++}-activated K^+ channel. *J. Gen. Physiol.* 90:427–449.

Montal, M. 1990. Molecular anatomy and molecular design of channel proteins. *FASEB J.* 4:2623–2635.

Murata, Y., H. Iwasaki, M. Sasaki, K. Inaba, and Y. Okamura. 2005. Phosphoinositide phosphatase activity coupled to an intrinsic voltage sensor. *Nature.* 435:1239–1243.

Nimigean, C.M., J.S. Chappie, and C. Miller. 2003. Electrostatic tuning of ion conductance in potassium channels. *Biochemistry.* 42:9263–9268.

Nimigean, C.M., T. Shane, and C. Miller. 2004. A cyclic nucleotide modulated prokaryotic K^+ channel. *J. Gen. Physiol.* 124:203–210.

Park, K.S., J.W. Yang, E. Seikel, and J.S. Trimmer. 2008. Potassium channel phosphorylation in excitable cells: providing dynamic functional variability to a diverse family of ion channels. *Physiology (Bethesda).* 23:49–57.

Pathak, M.M., V. Yarov-Yarovoy, G. Agarwal, B. Roux, P. Barth, S. Kohout, F. Tombola, and E.Y. Isacoff. 2007. Closing in on the resting state of the Shaker K(+) channel. *Neuron.* 56:124–140.

Patten, C.D., M. Caprini, R. Planells-Cases, and M. Montal. 1999. Structural and functional modularity of voltage-gated potassium channels. *FEBS Lett.* 463:375–381.

Ramsey, I.S., M.M. Moran, J.A. Chong, and D.E. Clapham. 2006. A voltage-gated proton-selective channel lacking the pore domain. *Nature.* 440:1213–1216.

Ruta, V., Y. Jiang, A. Lee, J. Chen, and R. MacKinnon. 2003. Functional analysis of an archaebacterial voltage-dependent K+ channel. *Nature.* 422:180–185.

Ruta, V., J. Chen, and R. MacKinnon. 2005. Calibrated measurement of gating-charge arginine displacement in the KvAP voltage-dependent K(+) channel. *Cell.* 123:463–475.

Saimi, Y., S.H. Loukin, X.L. Zhou, B. Martinac, and C. Kung. 1999. Ion channels in microbes. *Methods Enzymol.* 294:507–524.

Santos, J.S., A. Lundby, C. Zazueta, and M. Montal. 2006. Molecular template for a voltage sensor in a novel K^+ channel. I. Identification and functional characterization of KvLm, a voltage-gated K^+ channel from *Listeria monocytogenes. J. Gen. Physiol.* 128:283–292.

Sasaki, M., M. Takagi, and Y. Okamura. 2006. A voltage sensor-domain protein is a voltage-gated proton channel. *Science.* 312:589–592.

Schlosser, G., and G.P. Wagner. 2004. Modularity in Development and Evolution. The University of Chicago Press, Chicago. 600 pp.

Schoppa, N.E., and F.J. Sigworth. 1998a. Activation of shaker potassium channels. I. Characterization of voltage-dependent transitions. *J. Gen. Physiol.* 111:271–294.

Schoppa, N.E., and F.J. Sigworth. 1998b. Activation of Shaker potassium channels. II. Kinetics of the V2 mutant channel. *J. Gen. Physiol.* 111:295–311.

Schoppa, N.E., and F.J. Sigworth. 1998c. Activation of Shaker potassium channels. III. An activation gating model for wild-type and V2 mutant channels. *J. Gen. Physiol.* 111:313–342.

Schrempf, H., O. Schmidt, R. Kummerlen, S. Hinnah, D. Muller, M. Betzler, T. Steinkamp, and R. Wagner. 1995. A prokaryotic potassium ion channel with two predicted transmembrane segments from Streptomyces lividans. *EMBO J.* 14:5170–5178.

Seebohm, G., N. Strutz-Seebohm, O.N. Ureche, R. Baltaev, A. Lampert, G. Kornichuk, K. Kamiya, T.V. Wuttke, H. Lerche, M.C. Sanguinetti, and F. Lang. 2006. Differential roles of S6 domain hinges in the gating of KCNQ potassium channels. *Biophys. J.* 90:2235–2244.

Shapovalov, G., and H.A. Lester. 2004. Gating transitions in bacterial ion channels measured at 3 microns resolution. *J. Gen. Physiol.* 124:151–161.

Smith-Maxwell, C.J., J.L. Ledwell, and R.W. Aldrich. 1998a. Role of the S4 in cooperativity of voltage-dependent potassium channel activation. *J. Gen. Physiol.* 111:399–420.

Smith-Maxwell, C.J., J.L. Ledwell, and R.W. Aldrich. 1998b. Uncharged S4 residues and cooperativity in voltage-dependent potassium channel activation. *J. Gen. Physiol.* 111:421–439.

Swenson, R.P. Jr., and C.M. Armstrong. 1981. K+ channels close more slowly in the presence of external K+ and Rb+. *Nature.* 291:427–429.

Thompson, J.D., T.J. Gibson, F. Plewniak, F. Jeanmougin, and D.G. Higgins. 1997. The CLUSTAL_X windows interface: flexible strategies for multiple sequence alignment aided by quality analysis tools. *Nucleic Acids Res.* 25:4876–4882.

Yohannan, S., Y. Hu, and Y. Zhou. 2007. Crystallographic study of the tetrabutylammonium block to the KcsA K+ channel. *J. Mol. Biol.* 366:806–814.

Downloaded from http://rupress.org/jgp/article-pdf/132/6/651/1786737/jgp_200810077.pdf by guest on 09 February 2026

Zagotta, W.N., T. Hoshi, and R.W. Aldrich. 1994a. Shaker potassium channel gating. III: evaluation of kinetic models for activation. *J. Gen. Physiol.* 103:321–362.

Zagotta, W.N., T. Hoshi, J. Dittman, and R.W. Aldrich. 1994b. Shaker potassium channel gating. II: transitions in the activation pathway. *J. Gen. Physiol.* 103:279–319.

Zheng, J., and F.J. Sigworth. 1997. Selectivity changes during activation of mutant Shaker potassium channels. *J. Gen. Physiol.* 110:101–117.

Zheng, J., and F.J. Sigworth. 1998. Intermediate conductances during deactivation of heteromultimeric Shaker potassium channels. *J. Gen. Physiol.* 112:457–474.

Zheng, J., L. Vankataramanan, and F.J. Sigworth. 2001. Hidden Markov model analysis of intermediate gating steps associated with the pore gate of shaker potassium channels. *J. Gen. Physiol.* 118:547–564.

Zhou, Y., J.H. Morais-Cabral, A. Kaufman, and R. MacKinnon. 2001. Chemistry of ion coordination and hydration revealed by a K+ channel-Fab complex at 2.0 A resolution. *Nature.* 414:43–48.

Downloaded from http://rupress.org/jgp/article-pdf/132/6/651/1786737/jgp_200810077.pdf by guest on 09 February 2026